Targeting for success: mechanistic insights into microRNA-based gene therapy for Huntington disease
Sogorb Gonzalez, M.

Chapter 5

Beyond transduction:

Cross–corrective silencing of gene therapy through functional transfer of engineered microRNAs

Marina Sogorb-Gonzalez[1,2], Astrid Vallès[1], Zdenka Ellederova[3], Jan Motlik[3], Melvin Evers[1], Pavlina Konstantinova[1], Sander van Deventer[2]

[1] Department of Research and Development, uniQure biopharma B.V., Amsterdam

[2] Department of Gastroenterology and Hepatology, Leiden University Medical Center, Leiden, The Netherlands

[3] Institute of Animal Physiology and Genetics, Libechov, Czech Republic

Abstract

Adeno-associated virus (AAV)-based vectors are used to deliver gene therapies to brain cells in order to treat neurodegenerative diseases. Using this delivery technology, expression of the therapeutic transgene is limited to the cells that are primarily transduced by the AAV vector. In large animals, including humans, even the most advanced direct AAV administration technologies, such as intraparenchymal convention-enhanced delivery, will lead to transduction of a limited number of cells within a target brain area. Considering the extent of neuropathology of neurodegenerative diseases affecting most cells and multiple brain regions, widespread therapeutic targeting is needed for sufficient genetic correction. Extracellular vesicles (EV) are secreted nanovesicles that carry specific intracellular cargo and can transfer genetic information upon uptake by neighboring cells. In this study, we investigated the EV-mediated functional transfer of engineered microRNA (miRNA) molecules from AAV-corrected neuronal cells to neighboring cells. To investigate the secretion, uptake and gene-correction efficacy of engineered miRNAs mediated by EVs, we have set up *in vitro* cultures based on the co-culturing of human iPSC-derived neurons. The results demonstrated the transfer of engineered miRNAs and their ability to lower the expression of disease-causing genes upon transfer to recipient cells. Next, we analyzed the distribution of therapeutic miRNA in the brain of minipigs at 12 months after intrastriatal administration. In injected areas and anatomically connected regions, AAV vector DNA levels correlated with miRNA-induced protein lowering effect, while in non-directedly connected brain regions, we observed a mutant protein lowering effect in the presence of low or no vector DNA copies. Altogether our results indicate that AAV-delivered engineered miRNAs can disseminate to neighboring neuronal cells, potentially via EV, where they maintain its therapeutic effect in recipient cells. The spread of miRNA-based gene therapy, presumably mediated by EV, might be an effective mechanism to achieve greater therapeutic effect beyond transduction for gene therapies in neurodegenerative diseases.

5

Introduction

Huntington disease (HD) and spinocerebellar ataxia type 3 (SCA) are devastating neurodegenerative disorders triggered by triplet expansions in the huntingtin gene (*HTT*) and the ataxin 3 gene (*ATXN3*), respectively (MacDonald *et al.*, 1993; Kawaguchi *et al.*, 1994). The CAG repeat expansion results in the translation of an extended polyglutamine tract in the mutated protein which confers a toxic gain-of-function inducing misfolding and aggregation, cellular toxicity and neurodegeneration (Takahashi *et al.*, 2010). As a promising therapeutic approach for the treatment of HD and SCA*,* engineered microRNAs (miRNA) delivered by adeno-associated virus (AAV) (AAV-miRNA) have been designed to target the mutant mRNA and reduce the expression of the disease-causing proteins HTT and ATXN respectively (Miniarikova *et al.*, 2016; Martier *et al.*, 2019). Upon delivery of expression cassette into cell nucleus, precursor miRNAs are synthesized and processed into functional mature miRNAs by utilizing the cellular machinery of neuronal cells. Mature miRNAs are then loaded into the multiprotein RNA-induced silencing complex (RISC), which binds to the target mRNA inducing its degradation (Davidson and Boudreau, 2007). The expression of engineered miRNAs targeting *HTT* (miHTT) and *ATXN3* (miATXN3) mRNA transcripts has resulted in reduced levels of toxic mutant proteins in both in vitro and in vivo models (Miniarikova *et al.*, 2016, 2017; Keskin *et al.*, 2019; Martier *et al.*, 2019; Spronck *et al.*, 2019; Caron *et al.*, 2020; Valles *et al.*, 2021). Moreover, preclinical studies demonstrated a reduction of aggregate pathology, preservation of motor function and extension of survival (Miniarikova *et al.*, 2017; Martier *et al.*, 2019; Spronck *et al.*, 2019). In HD and SCA, as well as in most neurodegenerative diseases, the pathology and neuronal loss is initially limited to a defined brain region of selectively vulnerable neurons (Hobbs *et al.*, 2010). However, as disease progresses, broader depositions of pathological aggregates and neuronal dysfunction are found in numerous brain areas contributing to a progressive symptomatic decline. Considering the extend of neuropathology, one of the main challenges for gene therapies targeting the human central nervous system (CNS) is to achieve widespread distribution and sufficient levels of therapeutic molecules in all affected cells and regions of the brain after one-time administration.

Since the expression of therapeutic genes relies on the efficient AAV entry to neuronal cells, initial efforts have focused on optimizing AAV capsids and CNS delivery technologies. Capsid engineering via rational mutagenesis or directed evolution has been used to design vectors more capable of crossing blood-brain barrier, leading to better neuronal transduction after systemic administration (Deverman *et al.*, 2016; Chan *et al.*, 2017). Unfortunately, these results, initially demonstrated in C57BL/6 mice, did not translate to other larger species (Hordeaux *et al.*, 2018; Matsuzaki *et al.*, 2018). The site of injection and the AAV dose can also affect the dissemination of AAVs in the brain (Cearley and Wolfe,

5

2007, Samaranch *et al.*, 2017). Within the CNS parenchyma, AAVs can be transported from the site of injection via axonal pathways of the CNS connectome resulting in transduction at distal anatomically connected areas (Samaranch *et al.*, 2017). For instance, injection of AAV9 in brain areas with multiple dispersed projections, such as the ventral tegmental area, resulted in better distribution of the therapeutic gene compared to other brain areas with less projections, such as striatum or hippocampus (Cearley and Wolfe, 2007). Other attempts to potentiate AAV diffusion after local delivery in the brain include convection enhanced delivery (CED) via application of pressure differential (Hadaczek *et al.*, 2006), and co-infusion of factors such as heparin or mannitol (Mastakov *et al.*, 2002). Despite all these improvements, and using the best currently available AAV-based technologies, in large animals only a limited percentage of target cells is transduced by AAV vectors (Blits *et al.*, 2010). Therefore, mechanisms that contribute to the widespread diffusion of therapeutics beyond the initially transduced cells would promote removal of intracellular disease-inducing proteins in all affected neuronal cells and eventually prevent disease progression.

In this study, we propose a novel mechanism of dissemination of engineered miRNA therapeutics mediated by extracellular vesicles (EV), termed "*cross-corrective silencing*". EVs are membrane-delimited particles secreted by all cell types into extracellular space and carry important biological cargos including miRNAs. Circulating EVs are involved in distant inter-cellular communication by internalization in recipient cells, where upon endosomal escape, miRNA activity remains functional (Valadi *et al.*, 2007; Felicetti *et al.*, 2016). EVs are loaded with a selected subset of miRNAs, being miR-451 one of the most highly enriched in EVs compared to cellular levels (Guduric-Fuchs *et al.*, 2012). Moreover, siRNA sequences embedded into pre-miR-451 backbone were robustly packaged into secreted EV (Reshke *et al.*, 2020; Sogorb-Gonzalez *et al.*, 2021).

Here, we investigated functional transfer of engineered miRNAs, embedded into pre-miR-451 backbone, from AAV-corrected neuronal cells to neighboring cells. For this purpose, *in vitro* systems based on human neuronal cells differentiated from induced pluripotent stem cells (iPSC) were used. Following AAV transduction, dose-dependent levels of engineered miRNAs were detected in secreted EV-enriched fractions, which were then added to recipient cells demonstrating that EV-miRNA are taken up by recipient cells. Non-contacting co-culture of AAV-treated neurons together with non-treated cells resulted in gene silencing in both cultures, suggesting that engineered miRNAs remain functional upon internalization. Next, we analyzed the distribution patterns of therapeutic miRNAs in the large brain of minipigs at 12 months after intrastriatal administration of therapeutic AAV-miRNA (Valles *et al.*, 2021). In the injected areas (striatum) and the anatomically connected regions, AAV genomic levels correlated with miRNA-induced protein lowering effect. However, in non-directly connected brain regions, we observed a mild protein lowering effect in the presence of low or no vector DNA copies, which suggests a spread of

5

therapeutic efficacy beyond treated cells. Altogether, these results indicate that therapeutic miRNAs spread between neuronal cells, presumably via EV and exert therapeutic silencing of pathogenic proteins upon uptake in neighboring cells. Cross-corrective silencing of engineered miRNAs mediated EV might contribute to achieving widespread efficacy of gene therapeutics in CNS diseases.

Results

AAV-delivered engineered miRNAs are secreted by neuronal cells in a dose-dependent manner

Compared to other cellular miRNAs, miR-451 is one of the most highly packaged miRNAs within EVs (Guduric-Fuchs *et al.*, 2012; Reshke *et al.*, 2020). We hypothesized that engineered therapeutic miRNAs, embedded in a pre-miR-451 backbone, and expressed in neuronal cells might spread between cells in a similar manner as their endogenous counterparts, inducing a therapeutic gene correction in neighboring cells upon uptake (**Figure 1A**). In order to investigate the functional transfer of engineered miRNAs, we first evaluated the secretion levels of miRNAs by neuronal cells upon AAV-mediated expression. For this purpose, iPSC-derived neuronal cells were transduced with increasing doses of two therapeutic miRNAs deliver by AAV serotype 5 (AAV5): "miHTT", an engineered miRNA designed to target the exon 1 sequence of huntingtin (*HTT*) gene for Huntington disease (HD) (Miniarikova *et al.*, 2016), and "miATXN3", designed to target the ataxin 3 (*ATXN3*) gene for Spinocerebellar ataxia 3 (SCA3) (Martier *et al.*, 2019). Both engineered miRNAs were embedded in a pre-miRNA-451 scaffold. The processing, expression and efficacy have been previously tested both *in vitro* and in several animal models (Miniarikova *et al.*, 2017; Keskin *et al.*, 2019; Spronck *et al.*, 2019; Caron *et al.*, 2020). Following AAV-mediated transduction of neuronal cells and exhaustive washing, cell supernatants were collected and EV were isolated with an EV-specific precipitation buffer. EV-specificity was confirmed with specific markers and the EV yield was quantified as previously reported in our previous study (Sogorb-Gonzalez *et al.*, 2021). To quantify the intracellular and extracellular expression levels of engineered miRNAs, we used a TaqMan reverse transcription (RT)-quantitative (q)PCR with stem-loop primers specific for each mature miRNA sequence. AAV5-miHTT exposure dose-dependently increased both intracellular and well as extracellular levels of engineered miRNAs. Moreover, levels of intracellular transgene expression positively and significantly correlated with levels of extracellular miHTT enriched in EVs secreted from neuronal cells (**Figure 1B**). Similar results were obtained after transduction of iPSC-derived neuronal cells with AAV5-miATXN3, showing that intracellular

5

miATXN3 levels significantly correlated with extracellular levels of miATXN3 (**Figure 1C**). Hence, as previously demonstrated by us (Sogorb-Gonzalez *et al.*, 2021), engineered miRNAs expressed by neuronal are sorted and secreted within EVs in a dose-dependent manner.
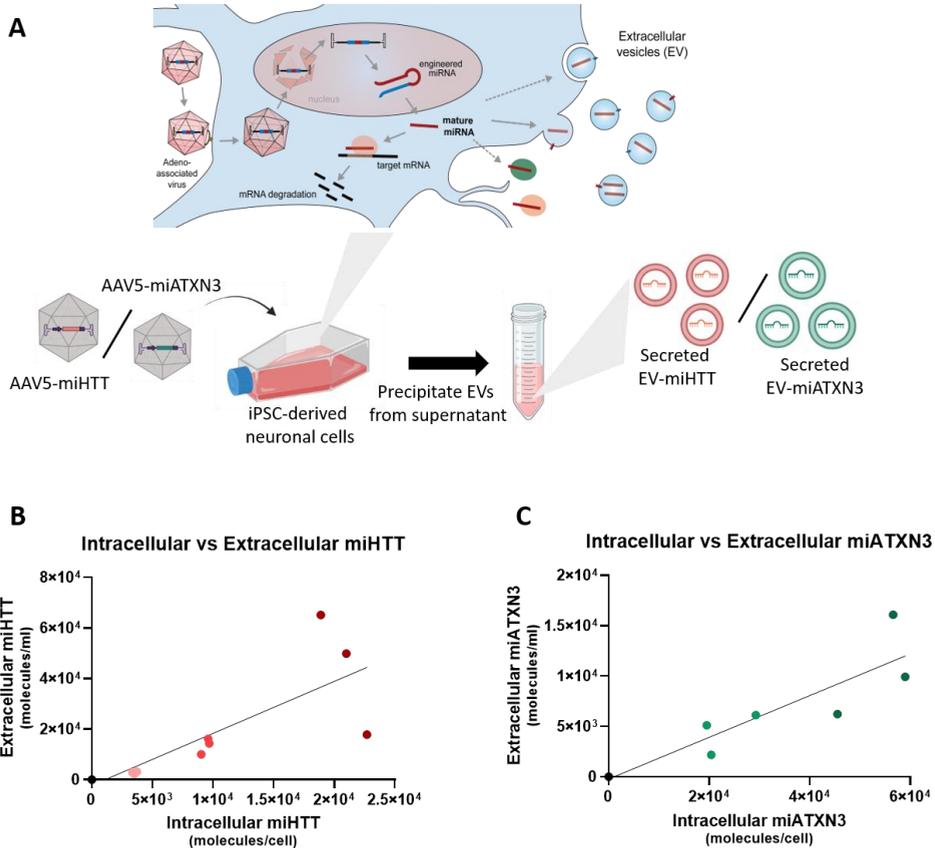

Figure 1. AAV-delivered artificial miRNAs are secreted by neuronal cells. A) Experimental outline shows transduction of iPSC-derived neuronal cells with either AAV5-miHTT or AAV5-miATXN3, collection of supernatant and precipitation of EVs enriched in miHTT and miATXN3 molecules respectively. **B)** Correlation analysis between intracellular miHTT levels (molecules/cell) in neuronal cells upon transduction with three increasing doses of AAV5-miHTT, and extracellular miHTT levels (molecules/ml) in supernatant medium (Simple linear regression, ***p=0.0014). **C)** Correlation analysis between intracellular miATXN3 levels (molecules/cell) in neuronal cells upon transduction with two increasing doses of AAV5-miATXN3, and extracellular miATXN3 levels (molecules/ml) in supernatant medium (Simple linear regression, ****p= 0.0006)

Engineered miRNAs enriched in EVs are taken up by recipient neuronal cells in a dose-dependent manner

To investigate whether engineered miRNAs enriched in EVs can be internalized by neighboring neuronal cells, we exposed non-treated neuronal cells to different concentrations of EVs secreted by AAV-transduced cells. EVs were precipitated from large volumes (1 ml to 10 ml) of supernatant of AAV-transduced neuronal cells with a precipitation buffer and centrifugation. To monitor the EV uptake, EVs were fluorescently tagged with PKH67 lipid-dye and then added to recipient neuronal cells (**Figure 2A).** An overlap between PKH67-EVs and cell membrane of recipient neuronal cells was observed at 24 hours after EV exposure, demonstrating the binding of EV to recipient cells (**Figure 2B**). Next, EVs precipitated from AAV5-miHTT transduced cells (EV-miHTT) and non-treated cells (EV-Ctrl) were added to naïve recipient cells in different concentrations (eg. 1x=1ml, 2x=2ml, 10x=10ml, 20x=20ml and 50x=50ml of supernatant). Since remaining AAV particles could also be enriched within EV fraction (not measured), miHTT levels in recipient cells were measured at 24h, hence prior to any potential transgene expression resulting from AAV contamination. At 24 hours after EV exposure, a dose-dependent increase of the intracellular miHTT concentration was detected in recipient cells (**Figure 2C**). Similarly, exposure of EVs precipitated from AAV5-miATXN3 transduced cells (EV-miATXN3) resulted in increasing levels of miATXN3 in recipient cells. (**Figure 2D**).
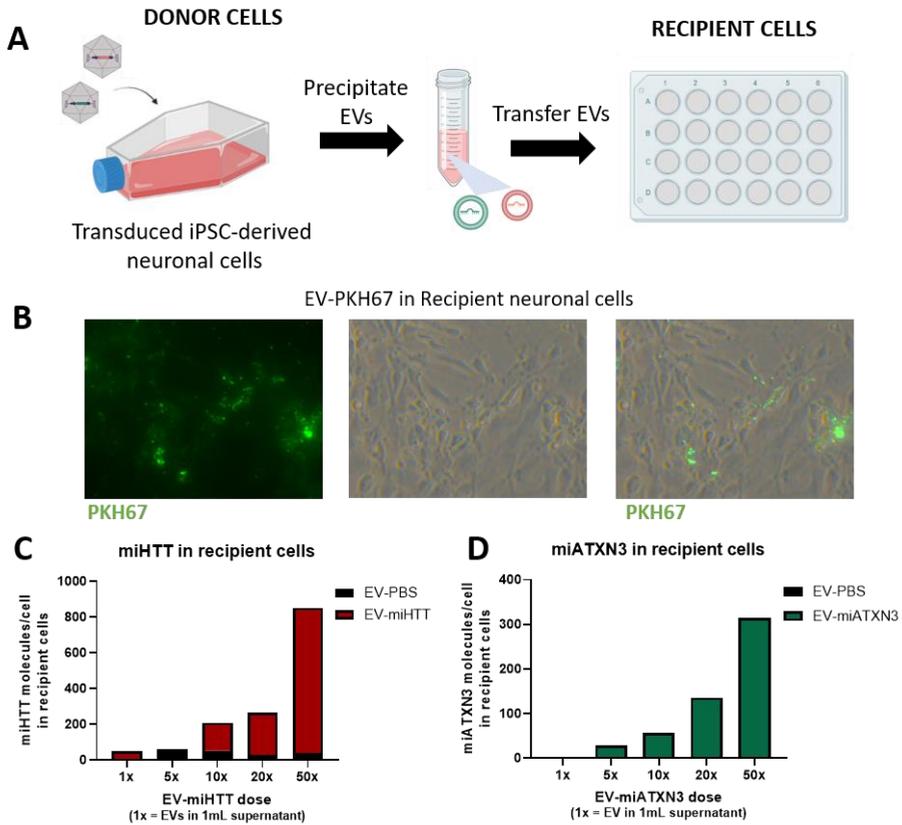
5

Figure 2. Engineered miRNAs enriched in EVs are taken up by recipient neuronal cells in a dose-dependent manner. A) Diagram of transduction of iPSC-derived neuronal cells with either AAV5-miHTT or AAV5-miATXN3, isolation of EVs by precipitation and exposure to recipient neuronal cells for 24 hours. **B)** Representative image of the uptake of PKH67 fluorescently-tagged EVs by recipient neuronal cells at 24h after EV exposure (dose = 20x EV or EV precipitated from 20ml of supernatant). **C)** Levels of engineered miHTT (molecules/cell) in recipient cells at 24 hours after exposure of increasing doses of miHTT-enriched EVs. Dose of "1x" equals amount of EVs present in 1ml supernatant of donor cells prior concentration and EV isolation. **D)** Levels of artificial miATXN3 (molecules/cell) in recipient cells at 24 hours after exposure of increasing doses of miATXN3-enriched EVs. Dose of "1x" equals amount of EVs present in 1ml supernatant of donor cells prior concentration and EV isolation.

Continuous transfer of engineered miHTT from AAV-treated neurons results in significant lowering of target *HTT* mRNA in recipient cells

Next, we investigated whether engineered miRNAs induce the degradation of target mRNA in recipient cells after EV transfer. Since the miRNA levels in recipient cells after one-time transfer were not sufficient to induce significant reduction of target transcript, we set up a cell culture assay that allows for continuous transfer of EV-miRNAs to recipient cells. For this, we used a transwell co-culture system in which AAV5-miHTT transduced "donor" cells were seeded in a transwell insert with a porous membrane and suspended in a standard tissue culture well containing non-treated "recipient" neuronal cells (**Figure 3A**). This system allows for the intercellular exchange of small secreted factors such as EVs while avoiding cell contamination or direct cell-to-cell contact. Two weeks after co-culture, cells within the different compartments were harvested with meticulous care to prevent cross-contamination and vector genomes were quantified in each cell population. We detected high numbers of AAV5 vector genome copies in AAV5-miHTT transduced "donor" cells by qPCR, but not in "recipient" cells or non-treated control cells (n=6) (**Figure 3B**), indicating a lack of viral transfer between donor and recipient cells. Next, levels of full-length *HTT* mRNA were measured by RT-PCR to quantify the efficacy of miHTT to reduce *HTT* expression upon AAV treatment or potential EV transfer. A 30% full-length *HTT* mRNA lowering was detected in AAV5-treated "donor" cells, when normalized to housekeeping gene *GAPDH* and compared to expression levels in control cells (n=6) (**Figure 3C**). Moreover, we measured a 20% *HTT* mRNA reduction in "recipient" cell co-cultured with AAV5-miHTT transduced cells for two weeks, presumably due to continuous transfer of miHTT molecules mediated by EV (**Figure 3C**). In contrast, gene expression levels of *ATXN3* and endogenous housekeeping genes were not affected (data not shown). Therefore, in the absence of vector DNA, a significant specific lowering of *HTT* expression was observed in recipient cells, indicating functional cross-corrective silencing by miHTT transfer.
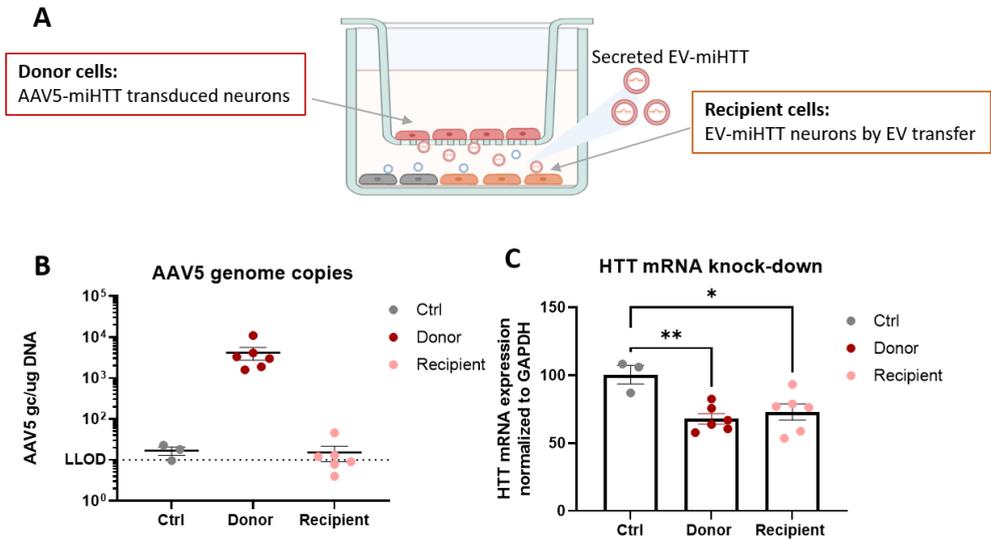
5

A

Donor cells:
AAV5-miHTT transduced neurons

Secreted EV-miHTT

Recipient cells:
EV-miHTT neurons by EV transfer

B AAV5 genome copies

C HTT mRNA knock-down

Figure 3. Non-viral continuous transfer of engineered miHTT enriched in EVs results in significant lowering of target *HTT* mRNA in recipient cells. A) Diagram of iPSC-derived neuronal cells cultured in a transwell co-culture system in which two cell compartment are separated by a filtered polyester membrane. Donor cells refer to neuronal cells transduced with high dose of AAV5-miHTT, washed and replated in upper compartment to ensure AAV removal. Recipient cells refer to naive neuronal cells seeded in the lower compartment. **B)** Quantification of AAV5 vector DNA levels (gc/µg DNA) in donor cells (AAV5-miHTT transduced) and recipient cells after 2 weeks of co-culture. Control cells are non-treated neuronal cells. Only donor cells had detectable levels of AAV5 genome copies. LLOD: lower limit of detection. **C)** Relative expression levels of target *HTT* mRNA from control cells and normalized to *GAPDH*. Significant lowering of *HTT* mRNA was detected in both donor and recipient cells after 2 weeks of co-culture (ANOVA, Tukey's multiple comparison test, *p=0.0197, **p=0.0197). Bars represent mean ± SEM.

5

Functional transfer of miATXN3-enriched EVs from transduced neuronal cells to recipient fibroblast cells

To further investigate the functional transfer of engineered miRNAs to neighboring cells, we set up a different non-contacting culture system based on the co-culture of non-chambered slides in a shared culture dish which allows for continuous transfer of secreted particles between two separated cell populations (**Figure 4A**). First, chambered cell culture slides were seeded with iPSC-derived neuronal cells and transduced with AAV5-miATXN3 for 5 days to ensure vector uncoating and transgene miATXN3 expression. To minimize the possibility of remaining AAV particles and subsequent cross-contamination, cells were carefully washed before chamber removal and transfer into the shared culture dish. To increase the transfer ratio, 3x slides containing AAV5-miATXN3 transduced neurons ("donor" cells) were co-cultured together with 1x separate slide containing non-treated fibroblasts ("recipient" cells). After 8 days, cells were separately harvested, and RNA was isolated for gene expression quantification by RT-qPCR. In concordance with previous studies (Martier 2019), neuronal cells directly transduced with AAV5-miATXN3 ("donor" cells) expressed high levels of miATXN3 molecules, up to 5×10^3 molecules/ng RNA (**Figure 4B**). Detectable levels of miATXN3, up to 1×10^2 molecules/ng RNA, were also found in "recipient" fibroblast cells, indicating the transfer and internalization of miATXN3 from AAV5-transduced to non-treated fibroblast cells (**Figure 4B**). As expected, a significant 43% reduction of *ATXN3* expression was detected in directly AAV5-treated neuronal cells ((**Figure 4C**). Moreover, a significant 22% lowering of *ATXN3* expression was also measured in "recipient" fibroblast cells after 8 days of co-culture (**Figure 4C**). In concordance to Figure 3, this data indicates that engineered miATXN3 molecules are transported, presumably within EVs, and taken up by recipient cells, where they maintain their therapeutic property in reducing *ATXN3* expression.
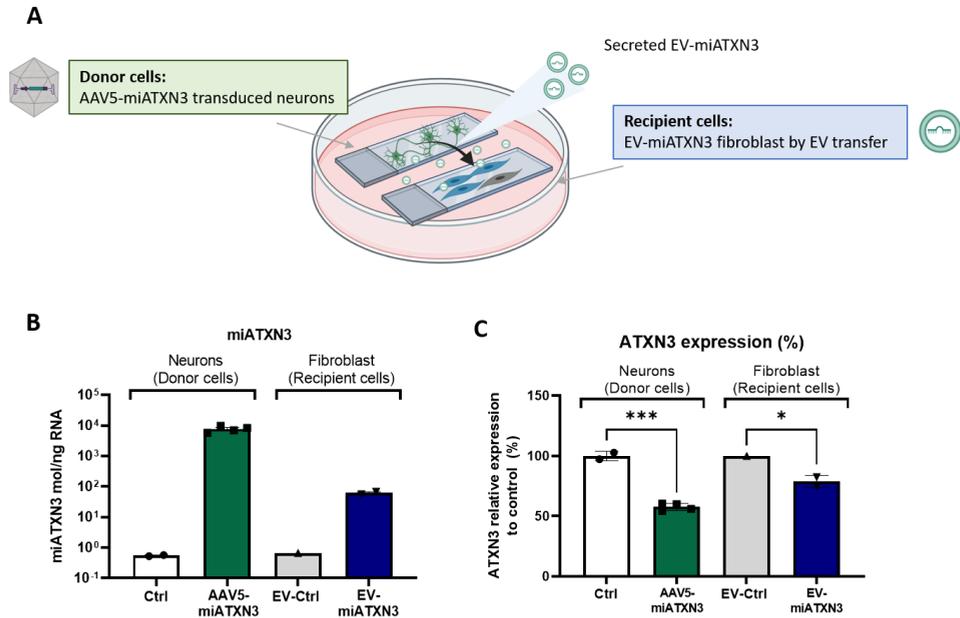
5

Figure 4. Functional transfer of miATXN3-enriched EVs from transduced neuronal cells to recipient fibroblast cells. A) Diagram of cell co-culture of iPSC-derived neuronal cells transduced with AAV5-miATXN3 (donor), and non-treated fibroblast (recipient), seeded in separate slides and co-culture in a tissue culture dish for 8 days. **B)** Quantification of miATXN3 molecules (molecules/ng RNA) in neuronal (donor) and fibroblast cells (recipient). Detectable levels were found in transduced neurons as well as in recipient fibroblast cells, likely due to EV-miATXN3 transfer during co-culture. **C)** Relative expression of target *ATXN3* mRNA compared to non-treated control cells and normalized to *GAPDH*. Significant lowering of *ATXN3* mRNA was detected in both transduced neuronal cells (43% lowering) and recipient fibroblast (22% lowering) after 8 days of co-culture. (ANOVA, Tukey's multiple comparison test, ***p=0.0002, *p=0.0205). Bars represent mean ± SEM.

Local AAV5-miHTT infusion in striatum results in widespread distribution and silencing efficacy

The striatum, composed by putamen and caudate, is the first and most affected area in HD patients (Hobbs *et al.*, 2010). The GABAergic medium spiny neurons (MSN) in the striatum receive projections from the cortex and thalamus, known as the "cortico-striatal-thalamic" pathway, as well as from substantia nigra pars compacta (SNc) (Zeun *et al.*, 2022). Striatal neurons send direct and indirect inhibitory projections to the globus pallidus and substantia nigra pars reticulata (**Figure 5B**).

We have previously demonstrated the biodistribution, efficacy and/or safety of AAV5-miHTT in several rodent models (Miniarikova *et al.*, 2017; Spronck *et al.*, 2019; Caron *et al.*, 2020), as well as in transgenic HD minipigs and in nonhuman primates (Evers *et al.*, 2018; Spronck *et al.*, 2021; Valles *et al.*, 2021). In these studies, intrastriatal administration of AAV5-miHTT resulted in widespread and persistent levels of vector DNA, miHTT transgene expression and mHTT lowering in the striatum, the main affected area in HD patient. As a consequence of anterograde and retrograde axonal transport of AAV5, vector genomes and *HTT* silencing were found in areas beyond the striatum, including cortex, thalamus, and globus pallidus, important areas also affected in HD. The axonal transport of AAV5 and other serotypes via the CNS circuitry has been previously described and is accepted to contribute to transgene distribution (Sondhi *et al.*, 2005; Cearley and Wolfe, 2007; Salegio *et al.*, 2013).

In a long-lasting study in HD transgenic minipig model (Baxa *et al.*, 2013), AAV5-miHTT striatal infusion resulted in a significant mHTT protein lowering in almost all brain areas (Valles *et al.*, 2021). Surprisingly, in some regions that contained low concentrations of vector DNA, mild reduction of mHTT protein was also observed. Our findings on the functional transfer of miHTT after AAV5-transduction suggested that, besides AAV axonal transport, the widespread mHTT lowering could be a result of EV-mediated spread of miHTT. This hypothesis is supported by the detection of circulating miHTT in the CSF of minipigs, as well as in nonhuman primates, up to two years after brain infusion (Sogorb-Gonzalez *et al.*, 2021; Valles *et al.*, 2021). To further investigate this proposition, we analyzed the spread of vector DNA and mHTT lowering effect in the different brain areas of HD transgenic minipigs at 12 months after AAV5-miHTT treatment. HD transgenic minipigs were treated with 1.2x10^13 gc of AAV5-miHTT per animal by bilateral injection in the putamen and caudate of each hemisphere (**Figure 5A**). The injection was performed by MRI-guided convention-enhanced delivery (CED) (Valles *et al.*, 2021). At 12 months after treatment, animals were sacrificed and tissues from multiple brain areas collected for molecular analysis. Areas were classified into directly connected and non-directly connected to the striatum according to the main basal ganglia pathways (**Figure 5B**). As expected, high levels of vDNA were measured in injected brain regions (caudate and

5

putamen) (**Figure 5C**). High vDNA concentrations were also measured in regions known to be directly connected to the striatum (thalamus, nucleus accumbens and cortex), while in non-directly connected areas (brain stem, hippocampus, and cerebellum) vDNA levels were low or below the limit of quantification (<5x10^3 gc/ug DNA) (**Figure 5C**). At 12 months after injection, significant region-dependent lowering of mHTT protein was measured in most brain areas with the exception of the cerebellum and spinal cord (data not shown), with an average 84% lowering in putamen (Valles *et al.*, 2 021). Correlation analysis showed a general significant negative correlation between mHTT levels (in % from control) and vDNA levels. (Pearson r -0.3260, p<0.0001) (**Figure 5C**). Interestingly, in some areas a significant mild reduction of mHTT protein (>25% lowering) was observed despite low levels of vector DNA (<1x10^4 gc/ug DNA) (blue shadowed area in Figure 5C).
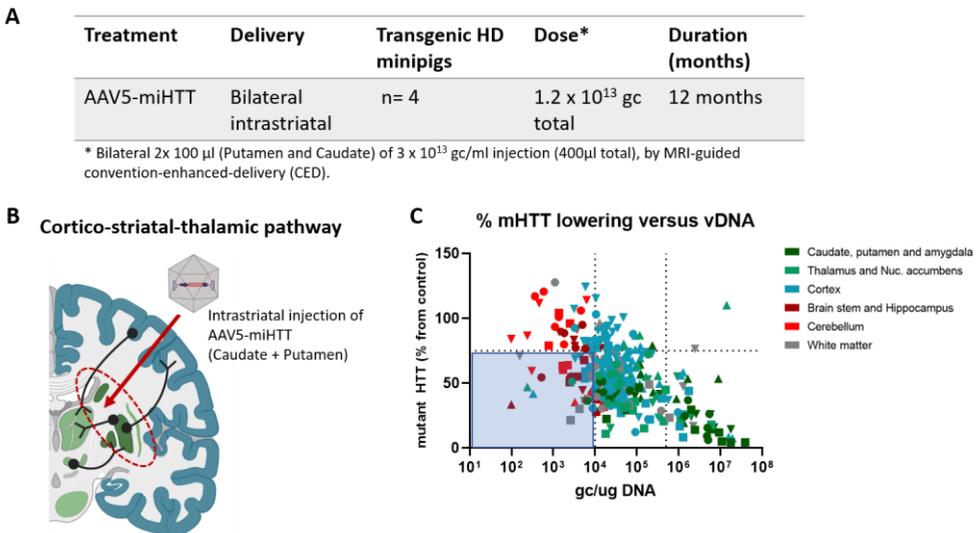

Figure 5. Intrastriatal delivery of AAV5-miHTT in transgenic HD minipigs results in widespread HTT lowering, even in regions with low concentrations of vector genomes (Valles et al 2020). A) Experimental design of minipig *in vivo* study. Four transgenic minipigs were injected with AAV5-miHTT by MRI-guided CED bilateral intrastriatal administration and sacrificed at 12 months post-injection (n=4). **B)** Diagram of injection location in striatum (caudate and putamen) and cortico-striatal-thalamic pathway showing direct connections between striatum (dark green), thalamus, substantia nigra (light green), and cortical areas (blue). **C)** Correlation analysis of mutant HTT protein (as % from non-treated controls) and AAV5 vector genome copies (gc/μg DNA) in different brain region of tgHD minipigs at 12 months post-injection of AAV5-miHTT in caudate and putamen. A significant negative correlation was obtained (Pearson r -0.3260, p<0.0001). Lines crossing the x-axis indicate the transduction threshold estimated to be needed for efficacy of HTT lowering (1x10^4 gc/μg DNA) and the minimum levels found in target areas (8x 10^5 gc/μg DNA). The line crossing the y-axis delimitates the efficacy threshold of 75% mutant HTT expression with respect to control. The blue shadowed region delimits the brain samples with vector DNA levels below the transduction threshold of 1x10^4 gc/ug DNA and mutant HTT protein levels below 75% from control.

Silencing efficacy is detected in distant non-directly connected brain areas

To investigate the contribution of *in vivo* cross-corrective silencing of miHTT between striatum and other directly and non-directly connected brain areas, we performed correlation analyses between vector distribution and HTT lowering for each brain area, depending on the direct or non-direct connections with the striatum. Significant correlations between AAV vDNA levels and mHTT lowering were found in the striatum (p<0.0001) (**Figure 6A**), as well as the in striatal-directly connected areas (thalamus, amygdala, nucleus accumbens and cortical regions) (p<0.0001) (**Figure 6B**). In contrast, non-significant correlation between vDNA levels and mHTT lowering was observed in non-directly-connected areas such as brain stem, hippocampus and cerebellum. In these areas, a substantial number of samples displayed >25% lowering of mHTT while levels of vDNA measured are considered too low to induce expression of therapeutic levels of miHTT. The same effect was measured when looking into cortical connections. Correlation analysis of cortical subregions showed a significant correlation between striatal-directly-connected cortical areas (prefrontal, motor, insular and perirhinal) (p=0.0007), but not between non-directly connected cortical regions (p=0.2831) (**Figure 6C**). These results indicate that while mHTT lowering might be induced by AAV transduction and axonal transport in directly-connected areas, while in other non-connected areas, reduction of mHTT protein is not explained by AAV levels and therefore, other mechanisms such as EV-spread might contribute to therapeutic lowering in these areas.
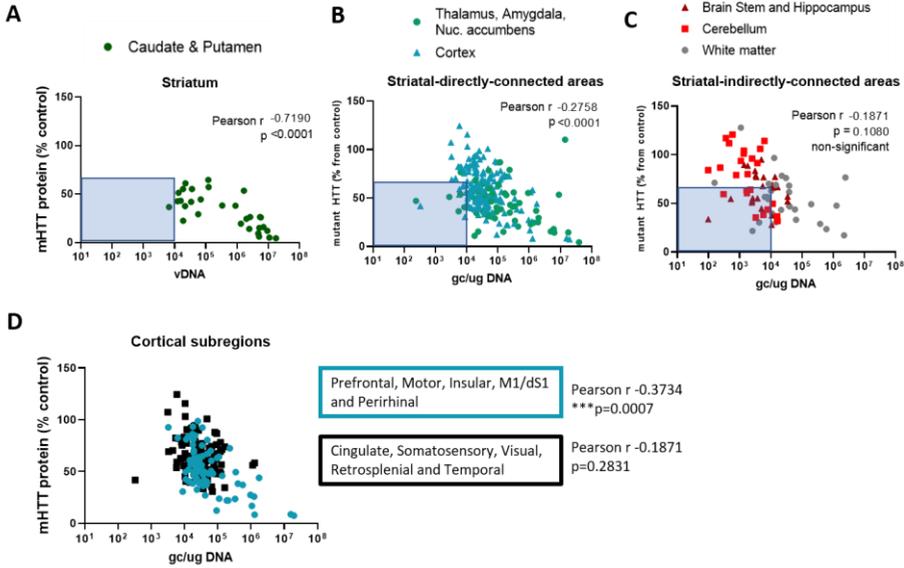
5

Figure 6. Lowering of mHTT protein in striatal-indirectly-connected brain areas does not correlate with AAV5 transduction levels. **A-C)** Mutant HTT protein levels (as % from control) in (A) striatum (injected region), (B) regions directly connected to striatum (thalamus, amygdala, nucleus accumbens and cortex) and (C) regions with indirect connections to striatum (brainstem, hippocampus, cerebellum and white matter). Pearson r correlations with AAV5 genome levels (gc/µg DNA) led to significant negative correlations in target regions (r -0.7190, ****p<0.0001) and directly connected regions (r - 0.2758, **** p<0.0001), but not in regions with indirect connections (r -0.1871, p=0.1080). **D)** Mutant HTT protein levels (as % from control) in subcortical regions with direct striatal connections (prefrontal, motor, insular somato-motor and perirhinal cortices), and with indirect striatal connections (cingulate, somatosensory, visual, retrosplenial and temporal cortices). Pearson correlations with AAV5 genome levels (gc/µg DNA) led to significant negative correlations in directly connected cortical regions (r -0.3734, p<0.0007) but not in subcortical regions with indirect striatal connections (r -0.1157, p=0.2831).

Discussion

The delivery and even biodistribution of therapeutic transgenes to all affected neurons and brain areas is one of the major challenges of gene therapy for neurodegenerative diseases. In HD, sufficient coverage of all striatal neurons, as well as cortical areas and thalamus, is thought to be required for therapeutic efficacy (Wang *et al.*, 2014). We demonstrated that AAV-delivered engineered miRNAs spread beyond treated neuronal cells to secondary neighboring and distant cells, presumably via EV. This mechanism of dissemination or cross-corrective silencing might contribute to the widespread brain distribution and efficacy of a promising AAV-mediated miRNA-based gene therapy for HD.

Previous studies have proposed and exploited the use of EVs as carriers of both endogenous or engineered miRNAs with therapeutic purposes. For instance, EVs collected from healthy donors, or siRNAs loaded in EVs have been studied as potential treatments for several diseases (Alvarez-Erviti *et al.*, 2011; Alexander *et al.*, 2015; Reshke *et al.*, 2020). However, due to their short half-life, repetitive administrations are required for sustained therapeutic effect, a significant disadvantage when targeting CNS diseases. In this study, we propose a novel role of EV as mediators of miRNA transfer inducing cross-corrective silencing. We hypothesized that AAV-transduced cells might become local "factories" of therapeutic engineered miRNAs, which will be then distributed to all affected neighboring cells resulting in a evenly and widely modulation of disease pathology. In order to better understand this process, we investigated the EV-mediated transfer of our therapeutic miRNAs in three distinct steps: (1) EV loading and secretion, (2) uptake by recipient cells and (3) *in vivo* gene-correction upon continuous transfer.

As a first step, we detected dose-dependent levels of engineered miRNAs in EV-enriched fractions after increasing doses of AAV-miRNA treatment, demonstrating the intracellular expression and subsequent secretion of our therapeutic miRNAs. Although these results may appear obvious, profiling studies have showed that EV-enriched miRNAs often differ from parent cells, indicating a regulated loading of miRNAs into EVs while others are retained within the cells (Guduric-Fuchs *et al.*, 2012; Squadrito *et al.*, 2014; Zhang *et al.*, 2015). One of the mechanisms involved in the sorting of miRNAs into EVs include Argonaoute-2 (Ago2) protein, an important component of pre-miRNA processing and functional RISC complex (McKenzie *et al.*, 2016). Ago2 is also involved in the processing of pre-miR-451, the only known miRNA which follows a dicer-independent non-canonical processing that relies on slicer activity by Ago2 protein (Cheloufi *et al.*, 2010; Herrera-Carrillo and Berkhout, 2017). Interestingly, miR-451 was consistently the most highly exported miRNA in different cell types (Guduric-Fuchs *et al.*, 2012), supporting the speculation that that the efficient EV export of miR-451 is mediated by Ago2. In this study, engineered therapeutic miRNAs (miHTT and miATXN3) were designed by embedding the

5

target sequence in a pre-miR-451 backbone. After AAV5 mediated delivery into neuronal cells, dose-dependent levels of therapeutic miRNAs were detected in EV-enriched vesicles. These findings are supported by our previous study, in which we detected circulating miHTT molecules in the CSF of minipigs and in nonhuman primates, up to two years after brain infusion (Sogorb-Gonzalez *et al.*, 2021; Valles *et al.*, 2021). This, together with the safe Dicer-independent processing, makes the selection of pri-miR-451 a suitable candidate for the design of miRNA-based therapeutics.

Second, the uptake of EV-enriched engineered miRNAs (miHTT and miATXN3) in recipient cells was demonstrated after one-time exposure with increasing levels of EV. In this experiment, EVs were specifically precipitated from the supernatant of AAV transduced cells and uptake was visualized by PKH67-membrane marker. Different pathways have been reported to mediate the internalization of EVs in recipient cells: clathrin-and caveolin-mediated endocytosis, phagocytosis and direct cell surface membrane fusion2 (Mulcahy *et al.*, 2014; O'Brien *et al.*, 2020). By silencing specific genes in recipient cells, de Jong et al. identified the important role of integrin ITGB1, Rab5 and Rab7 in endosome trafficking (de Jong *et al.*, 2020). The development of new sensitive and quantitative techniques might help to unravel the molecular mechanisms of EV binding and subsequent uptake in different biological systems (Toribio *et al.*, 2019; de Jong *et al.*, 2020). Moreover, the transfer by other potential carriers, such as lipoproteins or Ago2-bound complexes, remains to be investigated (Arroyo *et al.*, 2011).

Once inside the cells, miRNAs may either be degraded or remain active and induce gene silencing in recipient cells. To evaluate silencing efficacy upon transfer, we measured target engagement of *HTT* mRNA and *ATXN3* mRNA levels in recipient cells in a co-culture system with AAV-treated cells as donor cells. For this, a non-contacting co-culture that allows for a continuous transfer for 8-15 days was required to ensure sufficient levels of miRNA molecules and subsequent significant silencing in recipient cells. To exclude possible AAV-induced contamination among recipient cells and further characterize the mechanisms of secretion, future studies could include the development of a stable cell line overexpressing the engineered miRNAs as donor cells.

In vivo, in large HD transgenic minipig brains, we detected a widespread lowering effect after intrastriatal infusion, even in areas with low levels of AAV transduction. These findings, together with the *in vitro* functional transfer of engineered miRNAs, suggested that, besides AAV axonal transport, the widespread mHTT lowering could be a result of EV-mediated spread of miHTT. This hypothesis is supported by the detection of circulating miHTT in the CSF of treated animals up to two years after infusion (Sogorb-Gonzalez *et al.*, 2021; Valles *et al.*, 2021). The cross-corrective spread of therapeutic miRNAs after AAV-mediated expression might have some positive consequences for the treatment of HD and

other globally affected neurodegenerative diseases. In the striatum, the injected area, therapeutic miRNA transfer between neighboring neurons will result in a more equal therapeutic effect in all affected cells, instead of a potent lowering in AAV-target cells and no effect in neighboring cells. Hence, the AAV-target cells will become "local factories" of therapeutics to treat neighboring and distant cells. In other regions beyond striatum, affected in a later stage, minor secondary spread mediated by EV will contribute to therapeutic silencing and prevention of disease progression. Lowering of mHTT protein was not detected in spinal cord areas (Valles *et al.*, 2021), indicating that contribution of miRNA is still mild and safe. Moreover, the progression of HD from initially affected brain areas (striatum) to other regions (e.g cortex) is thought to be partially mediated by the EV transfer of mHTT fragments and aggregates (Jeon *et al.*, 2016; Tang, 2018). Assuming that the dissemination of therapeutic miRNAs within EV's would follow the same route as the pathological molecules, this might also contribute to a greater therapeutic effect.

Altogether, our findings indicate that engineered miRNAs embedded in pre-miR-451 scaffold, can be secreted, taken up and able to maintain its therapeutic properties in recipient cells, contributing to inter-cellular transfer and cross-corrective silencing effect in all affected neuronal cells beyond AAV transduction.

Material and methods

AAV production

AAV5 vector encoding cDNA of the miHTT cassette or miATXN3 was packaged into AAV5 by a baculovirus-based AAV production system (uniQure, Amsterdam, The Netherlands) as previously described (Evers *et al.*, 2018; Martier *et al.*, 2019).

Transduction and extracellular Vesicles (EVs) precipitation

Cells were transduced with different doses of AA5-miHTT ($3x10^{11}$ gc, $3x10^{12}$ gc and $3x10^{13}$ gc) at MOI $1x10^5$, $1x10^6$ and $1x10^7$ or AAV5-miATXN ($3x10^{12}$ gc and $3x10^{13}$ gc) at MOI $1x10^6$ and $1x10^7$. Medium from transduced neuronal cultures was refreshed every two days and collected on day 5 and day 12 after transduction, and centrifuged at 3000 x g for 15 min to remove cells and cell debris. The EVs were isolated with ExoQuick-TC (System Bioscience, California, USA) according to manufacturer's protocol. 3 ml of ExoQuick buffer was added to 10 ml of conditioned medium and incubated at 4°C overnight. Next day, the exosomes were collected at 1500 x g for 30 minutes and the supernatant was discarded. The residual solution was additionally centrifuged at 1500 x g for 10 minutes (Sogorb-Gonzalez *et al.*, 2021). The EVs pellets were re-suspended in appropriate buffers and stored at -80°C for further experiments.

Co-culture Transwell system

iPS-derived neuronal cells transduced with 3×10^{13} gc AAV5-miHTT were seeded in Coming® Transwell® polyester membrane cell culture inserts (24 mm, 0.4 pm pore, Sigma). Naive iPS-derived neurons were seeded 5×10^5 neurons/well in a 6-well plate. At 47 hours after seeding, inserts were placed on top of the wells and cells were cocultured for 2 weeks, refreshing medium every 2 or 3 days. Naive iPSC -derived cells without inserts were used as controls. Cells were harvested separately with Accutase (STEMcell technologies) and divided for further analysis.

Co-culture iPSC-derived neurons and fibroblast in chamber slides

Three-week matured iPSC-derived forebrain neurons from HD patient (Example 1) were plated in 4-well chamber slides in BrainPhys medium (StemCell technologies). Neuronal cells were transduced with a high dose of AAV-miATXN3 (1×10^{12} gc/well) at MOI 2×10^7. Five days after neuronal transduction, neuronal cells were properly washed, wells removed, and slides were placed into a petri dish (150mm) for co-culturing with non-transduced fibroblast cells. Fibroblast derived from human control individuals were purchased at Coriell repository. Cells were plated in 4 well chamber slides in MEM medium (Thermo Fisher) supplemented with 2 mM L-Glutamine, 15% Fetal Bovine Serum and 1% Penicillin/Streptomycin.

Co-culture system comprised of 3x transduced neuron slides and 1x non-transduced fibroblast slide (ratio 3:1) in MEM medium for 8 days. As a control, 3x non-transduced neurons slides were co-cultured with 1x non-transduced fibroblast slide in MEM medium. As a positive control, fibroblast cells were directly transduced with two doses of AAV-miATXN3 at MOI 1×10^6 and 1×10^8 and maintained for 8 days, likewise to the co-culture system (see Figure 4). Cells were washed, harvested separately and resuspend in 200ul Trizol for RNA purposes, or in 100ul RIPA buffer for protein assays, and stored at -80 C.

Minipig injections and sample collection (adapted from Valles et al. (Valles _et al._, 2021))

All experiments were carried out according to the guidelines for the care and use of experimental animals and approved by the State Veterinary Administration of the Czech Republic. TgHD minipigs (Baxa _et al._, 2013) and healthy controls of both sexes, 6 months old, were used. The animals were injected bilaterally into the caudate and putamen with a total of four catheters, one in each putamen and each caudate. Each minipig received 100 µl of 1.2×10^{13} gc/mL AAV-miHTT per catheter using the Renishaw drug delivery system. At 12 months after injection, n=4 treated animals and n=4 naïve (untreated) controls were sacrificed. From each of these animals, the brains were collected and sliced coronally (4 mm-thick sections) after which a total 170 brain punches of 3mm in diameter were taken bilaterally. Each punch of the left hemisphere was divided in four parts for different

purposes (DNA, RNA, protein or backup). All punches were kept at -80 C until further analysis.

RNA isolation and real-time qPCR

RNA was isolated from cells using Trizol according to the manufacturer's protocol (Invitrogen). To detect engineered miRNA expression levels, RT-qPCR was performed using TaqMan Fast Universal kit (Thermo Scientific), and commercially available primers and probes hsa-miR-16 (000391, Applied Biosystems). Custom-made miHTT primers and probes (assay ID CTXGPY4, Thermo Scientific) and miATXN3 primers and probes (assay ID CTEPRZE, Thermo Scientific), were used. The expression level was normalized to hsa-miR-16 levels. Fold changes of miRNA expression were calculated based on $2^{\wedge}\Delta\Delta CT$ method. miRNA expression was calculated based on a standard line with synthetic RNA oligos.

For the viral vector DNA isolation, neuronal cultures were processed using DNeasy Blood & Tissue Kit (Qiagen, Valencia, CA, USA) following manufacturer's protocol. AAV5 vector genome copies were measured by qPCR reaction using SYBR Green protocol (Applied Biosystems, Foster City, CA, USA) and validated standard line for detection of CAG promoter. Forward primer sequence: GAGCCGCAGCCATTGC and reverse primer sequence: CACAGATTTGGGACAAAGGAAGT. The standard line was used to calculate the genome copies per DNA microgram.

Statistical analysis

Statistical analysis and presented graphs were performed with GraphPad Prism 9 software. Data are expressed as means ± SEM. Correlation analysis were performed using liner regression analysis and Pearson's correlation as indicated. One-way ANOVA, with Tukey's multiple comparison's *post hoc* tests, was used for group comparison. The level of statistical significance was set at $p<0.005$ (*ns* non-significant, $*p<0.05$, $**p<0.005$, $***p<0.0005$, $****p<0.0001$).

5

References

Alexander M, Hu R, Runtsch MC, Kagele DA, Mosbruger TL, Tolmachova T, et al. Exosome-delivered microRNAs modulate the inflammatory response to endotoxin. Nat Commun 2015; 6: 7321.

Alvarez-Erviti L, Seow Y, Yin H, Betts C, Lakhal S, Wood MJA. Delivery of siRNA to the mouse brain by systemic injection of targeted exosomes. Nat Biotechnol 2011; 29: 341–5.

Arroyo JD, Chevillet JR, Kroh EM, Ruf IK, Pritchard CC, Gibson DF, et al. Argonaute2 complexes carry a population of circulating microRNAs independent of vesicles in human plasma. Proc Natl Acad Sci U S A 2011; 108: 5003–8.

Baxa M, Hruska-Plochan M, Juhas S, Vodicka P, Pavlok A, Juhasova J, et al. A transgenic minipig model of Huntington's Disease. J Huntingtons Dis 2013; 2: 47–68.

Blits B, Derks S, Twisk J, Ehlert E, Prins J, Verhaagen J. Adeno-associated viral vector (AAV)-mediated gene transfer in the red nucleus of the adult rat brain: comparative analysis of the transduction properties of seven AAV serotypes and lentiviral vectors. J Neurosci Methods 2010; 185: 257–63.

Caron NS, Southwell AL, Brouwers CC, Cengio LD, Xie Y, Black HF, et al. Potent and sustained huntingtin lowering via AAV5 encoding miRNA preserves striatal volume and cognitive function in a humanized mouse model of Huntington disease. Nucleic Acids Res 2020; 48: 36–54.

Cearley CN, Wolfe JH. A Single Injection of an Adeno-Associated Virus Vector into Nuclei with Divergent Connections Results in Widespread Vector Distribution in the Brain and Global Correction of a Neurogenetic Disease. J Neurosci 2007; 27: 9928–40.

Chan KY, Jang MJ, Yoo BB, Greenbaum A, Ravi N, Wu WL, et al. Engineered AAVs for efficient noninvasive gene delivery to the central and peripheral nervous systems. Nat Neurosci 2017; 20: 1172–9.

Cheloufi S, Dos Santos CO, Chong MMW, Hannon GJ. A dicer-independent miRNA biogenesis pathway that requires Ago catalysis. Nature 2010; 465: 584–9.

Davidson BL, Boudreau RL. RNA Interference: A Tool for Querying Nervous System Function and an Emerging Therapy. Neuron 2007; 53: 781–8.

Deverman BE, Pravdo PL, Simpson BP, Kumar SR, Chan KY, Banerjee A, et al. Cre-dependent selection yields AAV variants for widespread gene transfer to the adult brain. Nat Biotechnol 2016; 34: 204–9.

Evers MM, Miniarikova J, Juhas S, Vallès A, Bohuslavova B, Juhasova J, et al. AAV5-miHTT Gene Therapy Demonstrates Broad Distribution and Strong Human Mutant Huntingtin Lowering in a Huntington's Disease Minipig Model. Mol Ther 2018; 26: 2163–77.

Felicetti F, De Feo A, Coscia C, Puglisi R, Pedini F, Pasquini L, et al. Exosome-mediated transfer of miR-222 is sufficient to increase tumor malignancy in melanoma. J Transl Med 2016; 14: 56.

Guduric-Fuchs J, O'Connor A, Camp B, O'Neill CL, Medina RJ, Simpson DA. Selective extracellular vesicle-mediated export of an overlapping set of microRNAs from multiple cell types. BMC Genomics 2012; 13: 357.

Hadaczek P, Kohutnicka M, Krauze MT, Bringas J, Pivirotto P, Cunningham J, et al. Convection-enhanced delivery of adeno-associated virus type 2 (AAV2) into the striatum and transport of AAV2 within monkey brain. Hum Gene Ther 2006; 17: 291–302.

Herrera-Carrillo E, Berkhout B. Survey and summary: Dicer-independent processing of small RNA duplexes: Mechanistic insights and applications. Nucleic Acids Res 2017; 45: 10369–79.

Hobbs NZ, Barnes J, Frost C, Henley SMD, Wild EJ, Macdonald K, et al. Onset and progression of pathologic atrophy in Huntington disease: a longitudinal MR imaging study. AJNR Am J Neuroradiol 2010; 31: 1036–41.

Hordeaux J, Wang Q, Katz N, Buza EL, Bell P, Wilson JM. The Neurotropic Properties of AAV-PHP.B Are Limited to C57BL/6J Mice. Mol Ther 2018; 26: 664–8.

Jeon I, Cicchetti F, Cisbani G, Lee S, Li E, Bae J, et al. Human - to - mouse prion - like propagation of mutant huntingtin protein. Acta Neuropathol 2016; 132: 577–92.

de Jong OG, Murphy DE, Mäger I, Willms E, Garcia-Guerra A, Gitz-Francois JJ, et al. A CRISPR-Cas9-based reporter system for single-cell detection of extracellular vesicle-mediated functional transfer of RNA. Nat Commun 2020 111 2020; 11: 1–13.

Kawaguchi Y, Okamoto T, Taniwaki M, Aizawa M, Inoue M, Katayama S, et al. CAG expansions in a novel gene for Machado-Joseph disease at chromosome 14q32.1. Nat Genet 1994; 8: 221–8.

Keskin S, Brouwers CC, Sogorb-Gonzalez M, Martier R, Depla JA, Vallès A, et al. AAV5-miHTT Lowers Huntingtin mRNA and Protein without Off-Target Effects in Patient-Derived Neuronal Cultures and Astrocytes. Mol Ther - Methods Clin Dev 2019; 15: 275–84.

MacDonald ME, Ambrose CM, Duyao MP, Myers RH, Lin C, Srinidhi L, et al. A novel gene containing a trinucleotide repeat that is expanded and unstable on Huntington's disease chromosomes. Cell 1993; 72: 971–83.

Martier R, Sogorb-Gonzalez M, Stricker-Shaver J, Hübener-Schmid J, Keskin S, Klima J, et al. Development of an AAV-Based MicroRNA Gene Therapy to Treat Machado-Joseph Disease. Mol Ther - Methods Clin Dev 2019; 15: 343–58.

Mastakov MY, Baer K, Kotin RM, During MJ. Recombinant Adeno-associated Virus Serotypes 2– and 5–Mediated Gene Transfer in the Mammalian Brain: Quantitative Analysis of Heparin Co-infusion. Mol Ther 2002; 5: 371–80.

Matsuzaki Y, Konno A, Mochizuki R, Shinohara Y, Nitta K, Okada Y, et al. Intravenous administration of the adeno-associated virus-PHP.B capsid fails to upregulate transduction efficiency in the marmoset brain. Neurosci Lett 2018; 665: 182–8.

McKenzie AJ, Hoshino D, Hong NH, Cha DJ, Franklin JL, Coffey RJ, et al. KRAS-MEK Signaling Controls Ago2 Sorting into Exosomes. Cell Rep 2016; 15: 978–87.

Miniarikova J, Zanella I, Huseinovic A, van der Zon T, Hanemaaijer E, Martier R, et al. Design, Characterization, and Lead Selection of Therapeutic miRNAs Targeting Huntingtin for Development of Gene Therapy for Huntington's Disease. Mol Ther - Nucleic Acids 2016; 5: e297.

Miniarikova J, Zimmer V, Martier R, Brouwers CC, Pythoud C, Richetin K, et al. AAV5-miHTT gene therapy demonstrates suppression of mutant huntingtin aggregation and neuronal dysfunction in a rat model of Huntington's disease. Gene Ther 2017; 24: 630–9.

Mulcahy LA, Pink RC, Carter DRF. Routes and mechanisms of extracellular vesicle uptake. J Extracell Vesicles 2014; 3

O'Brien K, Breyne K, Ughetto S, Laurent LC, Breakefield XO. RNA delivery by extracellular vesicles in mammalian cells and its applications. Nat Rev Mol Cell Biol 2020 2110 2020; 21: 585–606.

Reshke R, Taylor JA, Savard A, Guo H, Rhym LH, Kowalski PS, et al. Reduction of the therapeutic dose of silencing RNA by packaging it in extracellular vesicles via a pre-microRNA backbone. Nat Biomed Eng 2020; 4: 52–68.

5

Salegio EA, Samaranch L, Kells AP, Mittermeyer G, San Sebastian W, Zhou S, et al. Axonal transport of adeno-associated viral vectors is serotype-dependent. Gene Ther 2013; 20: 348–52.

Samaranch L, Blits B, San Sebastian W, Hadaczek P, Bringas J, Sudhakar V, et al. MR-guided parenchymal delivery of adeno-associated viral vector serotype 5 in non-human primate brain. Gene Ther 2017; 24: 253–61.

Sogorb-Gonzalez M, Vendrell-Tornero C, Snapper J, Stam A, Keskin S, Miniarikova J, et al. Secreted therapeutics: monitoring durability of microRNA-based gene therapies in the central nervous system. Brain Commun 2021; 3

Sondhi D, Peterson DA, Giannaris EL, Sanders CT, Mendez BS, De B, et al. AAV2-mediated CLN2 gene transfer to rodent and non-human primate brain results in long-term TPP-I expression compatible with therapy for LINCL. Gene Ther 2005 1222 2005; 12: 1618–32.

Spronck EA, Brouwers CC, Vallès A, de Haan M, Petry H, van Deventer SJ, et al. AAV5-miHTT Gene Therapy Demonstrates Sustained Huntingtin Lowering and Functional Improvement in Huntington Disease Mouse Models. Mol Ther - Methods Clin Dev 2019; 13: 334–43.

Spronck EA, Vallès A, Lampen MH, Montenegro-Miranda PS, Keskin S, Heijink L, et al. Intrastriatal administration of AAV5-MIHTT in non-human primates and rats is well tolerated and results in MIHTT transgene expression in key areas of huntington disease pathology. Brain Sci 2021; 11: 1–18.

Squadrito ML, Baer C, Burdet F, Maderna C, Gilfillan GD, Lyle R, et al. Endogenous RNAs Modulate MicroRNA Sorting to Exosomes and Transfer to Acceptor Cells. Cell Rep 2014; 8: 1432–46.

Takahashi T, Katada S, Onodera O. Polyglutamine diseases: Where does toxicity come from? What is toxicity? Where are we going? J Mol Cell Biol 2010; 2: 180–91.

Tang BL. Unconventional Secretion and Intercellular Transfer of Mutant Huntingtin. Cells 2018; 7

Toribio V, Morales S, López-Martín S, Cardeñes B, Cabañas C, Yáñez-Mó M. Development of a quantitative method to measure EV uptake. Sci Reports 2019 91 2019; 9: 1–14.

Valadi H, Ekström K, Bossios A, Sjöstrand M, Lee JJ, Lötvall JO. Exosome-mediated transfer of mRNAs and microRNAs is a novel mechanism of genetic exchange between cells. Nat Cell Biol 2007; 9: 645–59.

Valles A, Evers MM, Stam A, Gonzalez MS, Brouwers C, Tornero CV, et al. Widespread and sustained target engagement in Huntington s disease minipigs upon intrastriatal microRNA-based gene therapy. Sci Transl Med 2021; 13: 1–51.

Wang N, Gray M, Lu XH, Cantle JP, Holley SM, Greiner E, et al. Neuronal targets for reducing mutant huntingtin expression to ameliorate disease in a mouse model of Huntington's disease. Nat Med 2014; 20: 536–41.

Zeun P, McColgan P, Dhollander T, Gregory S, Johnson EB, Papoutsi M, et al. Timing of selective basal ganglia white matter loss in premanifestHuntington's disease. Neuroimage (Amst) 2022; 33: 102927.

Zhang J, Li S, Mi S, Li L, Li M, Guo C, et al. Exosome and Exosomal MicroRNA : Trafficking , Sorting , and Function. Genomics, Proteomics Bioinforma 2015; 13: 17–24.

5